

Using Few-Shot Learning to Classify Primary Lung Cancer and Other Malignancy with Lung Metastasis in Cytological Imaging via Endobronchial Ultrasound Procedures

Ching-Kai Lin^{1,2,3,4}, Di-Chun Wei^{4*}, Yun-Chien Cheng^{4*},

¹ Department of Medicine, National Taiwan University Cancer Center, Taipei, Taiwan

² Department of Internal Medicine, National Taiwan University Hospital, Taipei, Taiwan

³ Department of Internal Medicine, National Taiwan University Hsin-Chu Hospital, Hsin-Chu, Taiwan

⁴ Department of Mechanical Engineering, College of Engineering, National Yang Ming Chiao Tung University, Hsin-Chu, Taiwan

*Corresponding author: yccheng@nycu.edu.tw, dichun.en11@nycu.edu.tw

Abstract

This study aims to establish a computer-aided diagnosis system for endobronchial ultrasound (EBUS) surgery to assist physicians in the preliminary diagnosis of metastatic cancer. This involves arranging immediate examinations for other sites of metastatic cancer after EBUS surgery, eliminating the need to wait for reports, thereby shortening the waiting time by more than half and enabling patients to detect other cancers earlier, allowing for early planning and implementation of treatment plans. Unlike previous studies on cell image classification, which have abundant datasets for training, this study must also be able to make effective classifications despite the limited amount of case data for lung metastatic cancer. In the realm of small data set classification methods, Few-shot learning (FSL) has become mainstream in recent years. Through its ability to train on small datasets and its strong generalization capabilities, FSL shows potential in this task of lung metastatic cell image classification. This study will adopt the approach of Few-shot learning, referencing existing proposed models, and designing a model architecture for classifying lung metastases cell images. Batch Spectral Regularization (BSR) will be incorporated as a loss update parameter, and the Finetune method of PMF will be modified. In terms of test results, compared to supervised learning and transfer learning methods, the PMF referenced in this study exhibits better feature extraction and classification capabilities, with an accuracy 10.6% and 6.2% higher, respectively, than those of supervised and transfer learning. This indicates that the use of FSL can better classify small datasets such as lung metastatic cancer cell images. Furthermore, the addition of BSR and the modified Finetune method further increases the accuracy by 8.89% to 65.60%, outperforming other FSL methods. This study confirms that FSL is superior to supervised and transfer learning in classifying metastatic cancer and demonstrates that using BSR as a loss function and modifying Finetune can enhance the model's capabilities.

Keywords: Cytological Imaging, deep learning, endobronchial ultrasound (EBUS), few-shot learning, lung metastasis, Vision Transformer

1. Introduction

Cancer is the leading cause of death in Taiwan, and the mortality rate has been increasing year by year. Early detection and treatment to reduce the mortality rate are key. With the prevalence of imaging examinations such as chest X-rays and computed tomography, lung lesions are becoming easier to detect. Besides primary lung cancer, the lungs are also a common site for metastasis

from other cancers. Cancer cells from other parts of the body often metastasize to the lungs, leading to an increase in mortality rates. The staging of primary lung cancer and cancers that have metastasized to the lungs varies significantly. In addition to having markedly different prognoses, different types of tumors require different choices of anti-tumor drugs. Therefore, obtaining specimens from lung lesions for diagnosis quickly and safely is crucial for the subsequent treatment plan for patients.

Endobronchial ultrasound (EBUS) is a relatively new minimally invasive technique for examining lung lesions. The surgical procedure involves using different ultrasound probes to locate lesions around the lungs or in the mediastinum/hilar region. Tissue specimens are obtained by slicing or puncturing, and rapid on-site cytologic evaluation (ROSE) is performed during the examination process. The freshly obtained tissue specimen is smeared onto a slide, quickly stained, and then examined under a microscope for cytologic image interpretation to confirm whether there is a sufficient slice specimen to improve the slice diagnostic rate. Finally, the collected specimens are sent to pathology for examination. After the pathology report is available, the subsequent treatment plan is carried out. If lung metastasis is found during this process, relevant examinations and treatments will be performed accordingly.

For the pathological results after EBUS slicing, it takes 3 to 7 working days to confirm. In addition, it takes several working days to confirm reports for examinations related to lung metastasis cancer. The total waiting time will be very long and inefficient, which can easily lead to cancer recurrence and endanger the patient's life. If cytologic images can be preliminarily interpreted during the EBUS examination process, relevant examinations for metastatic cancer can be arranged in advance, as shown by the orange line in Figure 1. This not only allows for early examinations but also enables the initiation of subsequent cancer-related treatment plans, significantly shortening the patient's treatment time and achieving early detection and early treatment. Since colorectal cancer and breast cancer are relatively common cancers that metastasize to the lungs, this study chooses these two types of lung metastatic cells and primary lung cancer cells as the subjects for deep network learning.

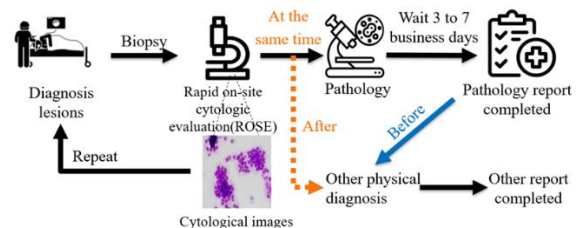


Figure 1: Workflow Differences with and without

Assistive Diagnosis

However, this study is expected to use only 400-500 cellular images, significantly fewer than the databases of other teams [4-8], such as 3012 images from the Wu team [4] and 4049 images from the Li team [5]. Therefore, it is not feasible to use the training models of other teams. It is necessary to select a training method suitable for a small amount of data. Common methods include few-shot learning [9-10], transfer learning [11], and Generative Adversarial Networks (GANs) [12]. Few-shot learning [10] involves training on very few data to generalize to new, unseen classes. Transfer learning [11] improves model performance by applying previously learned knowledge from one task to another related task. GANs [12] are used to generate synthetic data and improve model generalization. In this study, there are few cases of lung metastasis with a wide variety, requiring a robust and generalizable model. However, GANs generate images that are not real, raising concerns in medical applications, so this method is not adopted. Transfer learning requires a large amount of data and similar domain differences between the training and test sets, but there are few datasets similar to transfer cancer in reality, so this method is not adopted. Furthermore, this study requires a robust and generalizable model due to the small number of cases and the wide variety of data types. According to past literature, few-shot learning (FSL) has the advantages of using a small amount of data and strong generalization. Therefore, few-shot learning (FSL) is the main method of this study.

The methods of few-shot learning (FSL) [9] are divided into four types: Instance-guided Approaches, Parameter-based Approaches, Feature Post-processing Approaches, and Hybrid Approaches. Instance-guided Approaches aim to deepen the model's generalization ability through additional images. For example, the NSAE method proposed by the Liang team [13] uses reconstructed images as noise to enhance the model's learning. Parameter-based Approaches adjust the model's parameters to better fit the target dataset. For instance, the ReFine method proposed by the Oh team [14] initializes the last convolutional layer of the model before Finetuning the test set to avoid the model focusing too much on the training set, thereby updating the Finetune parameters to escape the training set's features and better fit the test set's features. Feature Post-processing Approaches process the original features to improve the classification prediction results. For example, the BSR method proposed by the Liu team [15] calculates the singular values of images as Loss calculation, which can prolong the model's training and increase its generalization ability. Hybrid Approaches combine the above methods to accomplish their respective tasks. This study will combine the above methods starting from the current baseline framework PMF [16] and design a model for classifying lung metastasis images.

The performance of deep learning architectures in analyzing cytological images has been validated in the cell image classification model. We have identified the following challenges in existing techniques:

- (1) No research has proposed effective methods to address the characteristics of lung metastatic cancer, such as multiple categories and few cases.
- (2) Previous methods mostly rely on sufficient datasets for model training. However, in cases where there are only small datasets for lung metastasis, there are no relevant classification methods or models available.

And the contributions of this study are summarized as follows:

- (1) Design a computer-aided diagnosis system that can classify different types of metastatic cancers to assist physicians in early detection and treatment for patients.
- (2) Develop a few-shot learning (FSL) model tailored to the characteristics of lung cancer cell images and lung metastasis cell images.

In summary, the goal of this study is to develop a computer-aided diagnostic system. The method proposed in this paper achieves higher performance compared to existing methods and reduces patient waiting time and advances diagnosis in clinical applications. The approach in this study aims to interpret images of lung metastasis cells, assisting physicians in interpreting cytological images and early detection of metastatic cancer types during examinations, ultimately improving patient survival rates.

2. Related Work

2.1. Few-Shot Learning (FSL)

Few-Shot Learning (FSL) [9] aims to learn from a limited amount of target data, which may or may not be consistent with the source data domain. The prediction strategy of FSL involves simulating the prediction process of the target data set by using a small amount of data from the source data set during training, creating a task for each training epoch. Multiple tasks are input to the model during each training epoch, and the parameters are updated after completing each task. After training, the model is used for predictions on the target data set. Multiple tasks are also created on the target data set for evaluating prediction results. Each task involves fine-tuning before testing the data set, and the final predictions are made by inputting the test set into the model.

In the terminology of FSL, as shown in Figure 2 [17], each task consists of two elements: the support set and the query set. The query set serves as the test set to evaluate the model's classification ability, while the

support set serves as the training set to train the model's classification ability. The term "N-way K-shot" indicates that in each task, the model is required to classify N classes, with K images provided for each class. The query set is a customizable set of images selected from each class for testing. By designing N-way K-shot tasks, FSL can achieve training and prediction on a limited amount of data in the target data set.



Figure 2. The data format of few-shot learning

3. Material and Methods

3.1. Dataset

The medical imaging dataset used in this study was provided by the Cancer Institute of National Taiwan University (IRB number: 202308088RINC), consisting of cytological images recorded during EBUS procedures. This study focuses on the classification of common metastatic cancers such as lung adenocarcinoma, breast cancer, and colorectal cancer. Therefore, the test set contains only cytological images of lung adenocarcinoma, breast cancer, and colorectal cancer.

3.2. Experimental Procedure

The experimental process is illustrated in Figure 4. This study begins with data collection, using the Mini-imagenet [18] public dataset for the training and validation sets, and medical images for the test set. For model design, the current Baseline model PMF [16] is modified and designed to create a model for classifying metastatic cancer cell images. Finally, the study conducts multiple tests, including:

- (1) Comparison of test results using various methods.
- (2) Comparison of test results using various models
- (3) Comparison between PMF and PMT
- (4) Comparison with and without using BSR

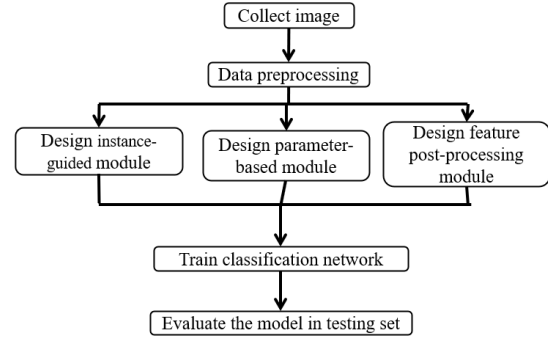


Figure 3. Experiment process

3.3. Data Preprocessing

Training set and validation set: The training set and validation set provided by the Mini-Imagenet public dataset [18] will be used. For model training, 500 training set tasks and 150 validation set tasks will be generated using the 5-way 5-shot method. For image processing, the training set will undergo data augmentation methods such as random cropping to 128x128, random changes in brightness, and horizontal flipping. The validation set will be resized to 128x128.

For the test set, to ensure that a single case does not appear in both the support set and query set simultaneously, this study will fixate on selecting 5 tasks. For each task, one case per class will be selected as the query set, and the unselected cases will be classified into the support set. The model's performance will be evaluated based on the average of the 5 task scores. The support set will randomly select 50 images per class using the 3-way 50-shot method. For image processing, the images will be resized to 147x147 and then center-cropped to 128x128.

3.4. Model Overview

The model designed in this paper is called BPMT, as shown in Figure 4. BPMT is a modification of the original PMF [16] architecture to meet the requirements of the task. It consists of three parts: the pre-training phase loads pre-trained parameters, followed by the meta-training phase where the model learns generalization, and finally the transfer learning phase where fine-tuning is performed for the task in this paper. The following describes these three stages in detail.

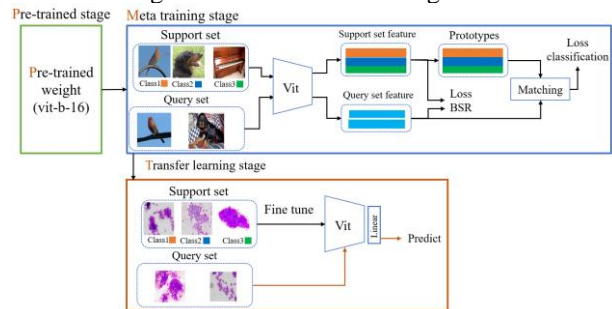


Figure 4. Overview of BPMT

3.4.1. Pre-trained stage

The pre-training phase aims to train a good model and apply it to the training phase to enhance the model's generalization ability. During this phase, many pre-trained weights are available online, such as those in Vit_b_16 which include pre-trained parameters like imagenet1k_v1[19],image21k[20],image1k_swag_e2e_v1 [19]. In this phase, the pre-trained parameters from image21k [20] as applied in the original PMF [16] will be used.

3.4.2. Meta training stage

The training phase aims to improve the model's generalization ability by training it on a small amount of data using a 5-way 15-shot approach to achieve classification. In the classifier, Prototype [21] is currently the best classifier, which works by taking the average of the features of the Support set images after they are passed through a vision transformer (ViT) and projected into a feature space, creating a class prototype. Finally, the Query set is projected into the feature space, and predictions are made based on the distance between each query and the class prototypes. The closer the distance, the higher the prediction likelihood for that class. In addition to the classification loss, the loss calculation also includes the BSR [15] loss, where the classification loss is the cross-entropy and the formula for the BSR loss [15] is as follows:

$$\ell_{bsr}(F(X)) = \sum_{i=1}^b \sigma_i^2 \quad (1)$$

Where σ represents the square of the singular values of image features. The overall loss is represented as follows:

$$\mathcal{L}_{total} = \ell_{cls}(C(X_Q), Y_Q) + \lambda \ell_{bsr}(F(X_Q, X_S)) \quad (2)$$

Where ℓ_{cls} is the classification loss, which calculates the cross-entropy between the model's predictions on the Query set and the actual labels. λ is a user-defined parameter. ℓ_{bsr} is the loss BSR [15], which computes the sum of the squared singular values of the features of each image.

3.4.3. Transfer learning stage

To better adapt to the current task, this paper will transfer the knowledge learned during the training phase of the model to the current task through transfer learning. The model will be fine-tuned to change the similarity calculation of the classifier from Prototype [21] to a fully connected layer for more precise prediction of the three categories. Before performing the prediction task, the model will be fine-tuned by adjusting the initial learning rate with a set of support sets to improve performance. After fine-tuning, the selected optimal initial learning

rate will be used for prediction on the query set.

3.5. Equipment

This experiment was conducted using an ASUS Z790-A GAMING WIFI 6E motherboard equipped with an Intel i9-13900K processor and an MSI RTX 4090 GAMING X TRIO 24G graphics card.

4. Result

4.1. Evaluation Methods

For the classification model, this study uses accuracy, precision, and recall as evaluation metrics. Accuracy is calculated as the number of correct answers divided by the total number of queries, expressed as a percentage. The formulas for precision and recall are as follows:

$$Precision = \frac{TP}{TP+FP} \quad (3)$$

$$Recall = \frac{TP}{TP+FN} \quad (4)$$

Among them, TP represents the number of correct predictions for that category, FP represents the number of predictions that are of the same category but actually belong to another category, and FN represents the number of instances that actually belong to the same category but are predicted by the model as another category. Precision and Recall represent the model's standards for correct or incorrect predictions for each class. The presented accuracy, precision, and recall are the average results for 5 sets of queries.

Since there are currently no other publicly available datasets related to transfer cancer, this study only uses data provided by a cancer specialist at National Taiwan University for testing purposes.

4.2. Implement detail

The hyperparameters used in training for this study include an initial learning rate of 5e-5, the optimizer being stochastic gradient descent (SGD), the classification loss function being Cross-entropy Loss, and parameter updates every 1 task. The total training consists of 200 epochs.

The hyperparameters used in fine-tuning for this study include an initial learning rate of 0.001, the optimizer being Adam, and the classification loss function being Cross-entropy Loss.

4.3. Comparison of different models

This section aims to compare few-shot learning methods with supervised learning methods and transfer

learning methods used for image classification. As shown in Table 1, the results of each method on the test set are presented, using the Vit_b_16 model as the main architecture, controlling for relevant training parameters, learning rate, and other conditions. The results indicate that among the few-shot learning methods used in this study, the accuracy is the highest and most indicators are superior to the other methods, indicating that using few-shot learning can effectively classify with a small amount of data.

Table 1. Comparison of different models

Method	Accuracy	Class0- Precision	Class1- Precision	Class2- Precision	Class0- Recall	Class1- Recall	Class2- Recall
Few-shot learning- PMF[16]	56.71%	0.6465	0.6267	0.4690	0.6024	0.6162	0.4771
Transfer learning	50.51%	0.6952	0.4275	0.4852	0.5229	0.3730	0.6195
Supervised learning	46.11%	0.4667	0.3657	0.6324	0.4381	0.6183	0.3996

4.4. Comparison of Various Models

This section aims to compare the method proposed in this study with current models in the field of few-shot learning. As shown in Table 2, the results of each method on the test set are presented. To ensure fairness, all methods use the Vit_b_16 model as the main architecture, with controlled conditions such as the number of ways, number of shots, training parameters, and learning rate. The results indicate that the method used in this study, BPMT, achieves the highest accuracy and outperforms other methods in most indicators, suggesting that the proposed approach can effectively classify the data in this study.

Table 2. Comparison of Various Models

Method	Accuracy	Class0- Precision	Class1- Precision	Class2- Precision	Class0- Recall	Class1- Recall	Class2- Recall
BPMT	65.60%	0.6331	0.7980	0.5720	0.5603	0.8333	0.5876
PMF[16]	56.71%	0.6465	0.6267	0.4690	0.6024	0.6162	0.4771
NSAE[13]	55.88%	0.5777	0.6882	0.4823	0.6429	0.4924	0.5528
ReFine[14]	56.94%	0.4815	0.7692	0.5391	0.5476	0.5210	0.6479

4.5. Comparison between PMF[16] and PMT

This section aims to explore the performance of simply modifying fine-tuning. As shown in Table 3, the performance of the modified PMT in various shot numbers compared to PMF [16] can be seen. It can be observed that the performance of PMT is better than PMF

[16]. This is because the classifier of PMT is a fully connected layer, which can address the drawback of PMF [16] that requires high model feature extraction capabilities for the prototype, resulting in better accuracy in classification. Therefore, the PMT method is more suitable for this study.

Table 3. Comparison between PMF[16] and PMT

Method	Shot	Accuracy	Class0- Precision	Class1- Precision	Class2- Precision	Class0- Recall	Class1- Recall	Class2- Recall
PMT	50	64.12%	0.5495	0.7919	0.6298	0.5849	0.7714	0.5878
PMF[16]	50	56.30%	0.6239	0.6397	0.4425	0.5579	0.6295	0.4981
PMT	20	64.03%	0.6657	0.6822	0.6054	0.5770	0.7114	0.6588
PMF[16]	20	52.78%	0.5436	0.6274	0.4217	0.5230	0.5648	0.4878
PMT	5	57.82%	0.5821	0.6828	0.4406	0.6294	0.6829	0.4447
PMF[16]	5	51.9%	0.5069	0.6468	0.4673	0.6341	0.5276	0.4100

4.6. Comparison with or without using BSR[15]

This section aims to investigate the performance of incorporating BSR loss [15]. As shown in Table 4, the performance of PMT with BSR [15] added is compared with PMT alone. It can be seen that the performance of PMT with BSR [15] added is better than PMT alone. This is because the singular values of BSR [15] focus on ensuring that the features on each image do not deviate too far from their original positions, thereby ensuring that the model's ability to extract features during training is not affected by parameter updates causing features to deviate too much from their original characteristics, leading to better extraction of image features. Therefore, the BSR [15] method is also applicable to this study.

Table 4. Comparison with or without using BSR[15]

Method	Accuracy	Class0- Precision	Class1- Precision	Class2- Precision	Class0- Recall	Class1- Recall	Class2- Recall
PMT	64.12%	0.5495	0.7919	0.6298	0.5849	0.7714	0.5878
PMT+BSR	65.60%	0.6331	0.7980	0.5720	0.5603	0.8333	0.5876

5. Conclusion

In the current study, the proposed BPMT model achieved an accuracy of 65.60% in predicting the transfer cancer type in the test set of cell images. Both precision and recall were improved to above 0.55, with some categories reaching 0.8333. Changing the classifier reduces the model's requirement for feature extraction, and incorporating the BSR[15] method improves the model's feature capturing ability. Compared to other methods, the proposed model performs the best.

There is still room for improvement in the proposed model. Future work could include incorporating the prediction of local features during model training to

increase the model's sensitivity to extracting fine features of local characteristics. Additionally, techniques such as data augmentation could be added during fine-tuning to improve the model's performance and generalization ability after fine-tuning. However, there are limitations to this study. The dataset used in this study is from the same hospital, and the number of cases is quite rare. Differences in cases and equipment between different hospitals will cause differences in the quality of cytological images, which will affect the model's prediction ability. The model may be inaccurate or not applicable to other hospital datasets when predicting on other data. In the future, it is hoped that more training data can be obtained to allow the model to learn more relevant features of cancer cells, thereby improving model performance, robustness, and generalization.

6. Reference

- [1]. <https://dep.mohw.gov.tw/dos/lp-5069-113.html>
- [2]. <https://www.skh.org.tw/skh/ea8b54b315.html>
- [3]. Lin et al. Rapid on-site cytologic evaluation by pulmonologist improved diagnostic accuracy of endobronchial ultrasound-guided transbronchial biopsy. *Formos Med Assoc.* 2021 Jun;120(6):1414-1415.
- [4].Miao Wu, Chuanbo Yan, Huiqiang Liu, Qian Liu, Yi Yin; Automatic classification of cervical cancer from cytological images by using convolutional neural network. *Biosci Rep* 21 December 2018; 38 (6): BSR20181769.
- [5].Li, J., Dou, Q., Yang, H., Liu, J., Fu, L., Zhang, Y., ... & Zhang, D. (2022). Cervical cell multi-classification algorithm using global context information and attention mechanism. *Tissue and Cell*, 74, 101677.
- [6].Dimauro, G., et al., Nasal cytology with deep learning techniques. *International journal of medical informatics*, 2019. 122: p. 13-19.
- [7].Shi, J., et al., Cervical cell classification with graph convolutional network. *Computer Methods and Programs in Biomedicine*, 2021. 198: p. 105807.
- [8]. Bakht, A.B., et al. Thyroid nodule cell classification in cytology images using transfer learning approach. in *Proceedings of the 12th International Conference on Soft Computing and Pattern Recognition (SoCPaR 2020)* 12. 2021. Springer.
- [9].Xu, H., et al., Deep Learning for Cross-Domain Few-Shot Visual Recognition: A Survey. *arXiv preprint arXiv:2303.08557*, 2023.
- [10]. Wang, Y., Yao, Q., Kwok, J. T., & Ni, L. M. (2020). Generalizing from a few examples: A survey on few-shot learning. *ACM Computing Surveys (CSUR)*, 53(3), 1–34.
- [11]. Weiss, K., T.M. Khoshgoftaar, and D. Wang, A survey of transfer learning. *Journal of Big data*, 2016. 3(1): p. 1-40.
- [12]. Wang, Z., Q. She, and T.E. Ward, Generative adversarial networks in computer vision: A survey and taxonomy. *ACM Computing Surveys (CSUR)*, 2021. 54(2): p. 1-38.
- [13]. Liang, H., et al. Boosting the generalization capability in cross-domain few-shot learning via noise-enhanced supervised autoencoder. in *Proceedings of the IEEE/CVF International Conference on Computer Vision*. 2021.
- [14]. Oh, J., et al. ReFine: Re-randomization before Fine-tuning for Cross-domain Few-shot Learning. in *Proceedings of the 31st ACM International Conference on Information & Knowledge Management*. 2022.
- [15]. Liu, B., et al., Feature transformation ensemble model with batch spectral regularization for cross-domain few-shot classification. *arXiv preprint arXiv:2005.08463*, 2020.
- [16]. Hu, S.X., et al. Pushing the limits of simple pipelines for few-shot learning: External data and fine-tuning make a difference. in *Proceedings of the IEEE/CVF Conference on Computer Vision and Pattern Recognition*. 2022.
- [17]. <https://www.borealisai.com/research-blogs/tutorial-2-few-shot-learning-and-meta-learning-i/>
- [18]. Oriol Vinyals, Charles Blundell, Timothy Lillicrap, Koray Kavukcuoglu, and Daan Wierstra. Matching networks for one shot learning. In *NeurIPS*, 2016. 1, 3, 5
- [19]. https://pytorch.org/vision/main/models/generated/torchvision.models.vit_b_16.html
- [20]. https://github.com/google-research/vision_transformer
- [21]. J. Snell, K. Swersky, and R. S. Zemel. 2017. Prototypical networks for few-shot learning. In *Advances in Neural Information Processing Systems*. 4077–4087.